

EXTENSIVE SET OF LOW-FIDELITY COVARIANCES IN FAST NEUTRON REGION

M.T. Pigni, M. Herman, P. Obložinský, D. Rochman

National Nuclear Data Center, Brookhaven National Laboratory, Upton, New York 11973-5000

An extensive set of covariances for neutron cross sections has been developed to provide initial, low-fidelity but consistent uncertainty data for nuclear criticality safety applications. The methodology for the determination of such covariances in fast neutron region is presented. It combines the nuclear reaction code EMPIRE, which calculates sensitivity to nuclear reaction model parameters and the Bayesian code KALMAN to propagate uncertainty of the model parameters onto cross sections. Taking into account the large scale of the project (219 fission products), only partial reference to experimental data has been made. Therefore, the covariances are, to a large extent, derived from the perturbation of several critical model parameters selected through the sensitivity analysis. They define optical potential, level densities and pre-equilibrium emission. This exercise represents the first attempt to generate nuclear data covariances on such a scale.

I. INTRODUCTION

Several advanced nuclear systems and fuel cycles are being evaluated in a number of current programs at the DOE-NE (e.g., GNEP, GEN-IV, and the Advanced Fuel Cycle Initiative - AFCI). Advanced nuclear concepts are being considered with fuel and reactor characteristics that are well outside the design envelope of existing and prior systems. Unfortunately, only small perturbations in design features from those in existing systems can be determined with high confidence using available nuclear data libraries. Therefore, a wide effort for advanced simulations foreseen within GNEP must be preceded with the adequate adjustment of the recently released ENDF/B-VII.0 library¹ to the integral experiments that are suitable for constraining nuclear data to the particular design features of the new systems. Nuclear data covariances (uncertainties and correlations) are essential for such adjustment. They also are of key importance for development, optimization and long-term deployment of innovative energy systems (GNEP) and associated fuel cycles (AFCI). They allow for reactor sensitivity analyzes, design studies and estimation of the reactor parameter margins.

Current availability of covariances in the major nuclear data libraries is very limited. The most recent ENDF/B-VII.0 library, released in December 2006, contains covariances for 26 materials², i.e., for less than 7% of the materials included in the neutron sub-library. Only half of them covers all reaction channels important for applications and can be, therefore, considered complete. Lack of a consistent and complete set of covariances is a barrier that prevents using the sensitivity tools in the development of innovative nuclear technologies and discourages advancement of the tools themselves. The goal of the ‘low-fidelity covariance project’ is to produce rough set of covariances covering all relevant reaction channels and materials to provide a solid base for testing the new tools for advanced numerical simulations employing nuclear data uncertainties and correlations. Accordingly, the emphasis of the low-fidelity project is on the completeness rather than on the precision - the latter should come later once the technology is well established and adequate methods made available.

BNL and LANL took lead of the ‘low-fidelity’ project in the fast neutron region ($5 \text{ keV} \leq E \leq 20 \text{ MeV}$). The methodology used in the present work is based on the BNL nuclear reaction code EMPIRE³ and Bayesian filter code KALMAN⁴ (LANL). Apart from actinides and light nuclei, the present work intends to provide covariance information for the remaining 304 materials in the new ENDF/B-VII.0 library (see Tab. I).

Table I. List of 304 materials to be evaluated by BNL. It corresponds to the Neutron Sub-library present in ENDF/B-VII.0.

Type	Nuclei	No. of isotopes
Structural nuclei	¹⁹ F - ^{nat} Zn	57
Fission products	⁶⁹ Ga - ¹⁷⁰ Er	219
Heavy nuclei	¹⁷⁵ Lu - ²⁰⁹ Bi	31

In view of the large scale of the present project, the results are fully based on model calculations without reference to experimental data. The EMPIRE code calculations with default set of parame-

ters provide a complete set of cross sections, while the KALMAN code generates their (co)variances. We stress, that the EMPIRE results, although reasonable for many major channels, do not coincide with any of the official evaluated libraries. Therefore, the obtained covariances are not intended to be associated with any cross sections recommended for applications. Total neglect of the experimental data, and global character of the model calculations also prevent any meaningful comparison with the existing covariances that result from a much more thorough analysis. In Section II, we present the general concept of the procedure to determine uncertainties and related covariance matrices. Section III gives an overview of model parameters to which calculated cross sections are most sensitive. The results and the applicability of the method is demonstrated in Section IV, while conclusions on the predictive power and open questions are discussed in Section V.

II. EVALUATION METHOD

The *EMPIRE-KALMAN* method combines physics modeling of nuclear reactions with the Bayesian update procedure, which is a standard tool used in statistics to evaluate the effect of the new data. The evaluation starts with the *EMPIRE* nuclear reaction model code which makes use of a wide range of nuclear models of different degree of sophistication in order to provide an overall description of nuclear observables. The models applied are address specific reaction mechanisms and are characterized by adjustable parameters. The most relevant model parameters are those related to optical potential and nuclear level densities. These parameters are varied to calculate partial derivatives of cross sections defining elements of the sensitivity matrices (e.g. Eq. 3). Thus, the reaction cross sections, sensitivity matrices and the list of model parameters with relative uncertainties are input quantities for the *KALMAN* code. This code is used as a nuclear data evaluation tool based on the iterative least-square approach. The procedure puts emphasis on the estimation of the model parameter uncertainties and the corresponding correlations. The procedure is then applied to the evaluation of neutron cross sections and their covariance matrices for various reaction channels. The application of the Bayesian equations is straightforward and the update is a simple algebraic operation,

$$\mathbf{x}^{(n+1)} = \mathbf{x}^{(n)} + \mathbf{X}^{(n)} \mathbf{A}^T \mathbf{Q}^{(n)} (\boldsymbol{\eta}^{(n)} - \boldsymbol{\sigma}(\mathbf{x}^{(n)}))$$

$$\mathbf{X}^{(n+1)} = \mathbf{X}^{(n)} - \mathbf{X}^{(n)} \mathbf{A}^T \mathbf{Q}^{(n)} \mathbf{A} \mathbf{X}^{(n)}, \quad (1)$$

where n denotes the n^{th} -step in the evaluation process according to the number of sets of experimental

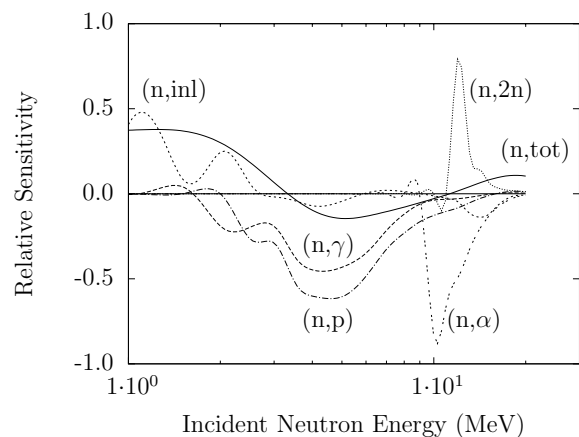


Fig. 1. Energy dependence of the relative sensitivity to V_v for the most important neutron induced reactions on ^{89}Y . V_v has been varied by $\Delta V_v = \pm 5\%$ (see Eq. 4).

data to be included. The vector $\mathbf{x}^{(n+1)}$ contains the improved values of the parameters starting from the vector $\mathbf{x}^{(n)}$. Likewise, the matrix $\mathbf{X}^{(n+1)}$ is the updated covariance matrix of the parameters $\mathbf{x}^{(n+1)}$. The combination between experimental and theoretical covariance matrices results in the updated error matrix, $\mathbf{Q} = (\mathbf{W} + \mathbf{V})^{-1}$, where \mathbf{V} is the covariance matrix corresponding to the experimental cross sections $\boldsymbol{\eta}$. The vector $\boldsymbol{\sigma}(\mathbf{x})$ represents the set of cross sections for a specific reaction channel (total, elastic, capture, ...) calculated for the set of parameters \mathbf{x} . The corresponding covariance matrix,

$$\mathbf{W} = \mathbf{A} \mathbf{X} \mathbf{A}^T \quad (2)$$

is associated with a model calculation by the correlation matrix of the model parameters, $\mathbf{X} \equiv \langle \Delta x_\ell \Delta x_m \rangle$, and the sensitivity matrix \mathbf{A} with elements,

$$a_{i,j} = \frac{\partial \sigma(\mathbf{x}, E_i)}{\partial x_j}. \quad (3)$$

calculated at the energy E_i .

III. MODEL PARAMETERS

EMPIRE code system is a modern tool for modeling nuclear reactions, which is mainly used for data evaluations. The code incorporates an extended set of nuclear reaction models capable of simulating all relevant reaction mechanisms. Therefore, *EMPIRE* provides reasonable overall description of nuclear observables even if default parametrization is being used. The advantage of *EMPIRE* is the simplicity of the input, default values for all parameters and wide

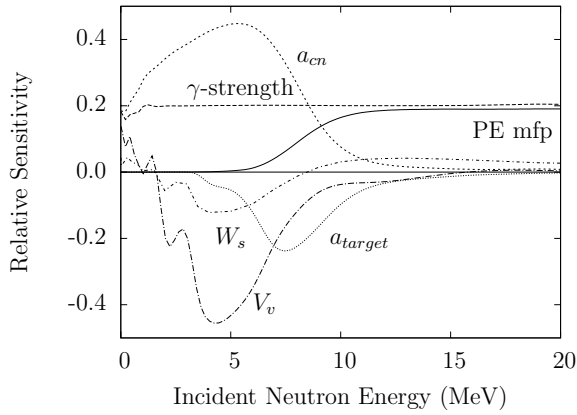


Fig. 2. Relative sensitivity of the $^{89}\text{Y}(n,\gamma)$ reaction, to the perturbation of level density and optical model parameters by $\pm 5\%$ and γ -ray as well as pre-equilibrium strength by $\pm 10\%$.

range of target mass number ($A \geq 19$) and incident energies.

For the purpose of this project, the adjustable parameters are limited to the ones listed in Tabs. II and III. These parameters are expected to contribute significantly to the cross section uncertainties. The effect of a perturbation of a model parameter on cross sections is determined via the relation

$$\mathcal{S}_\rho(E, k) = \frac{\sigma_\rho^{(+)}(E, k) - \sigma_\rho^{(-)}(E, k)}{\sigma_\rho^{(0)}(E)}, \quad (4)$$

where,

$$\sigma_\rho^{(0)}(E) = \sigma_\rho(E; x_1, \dots, x_j)$$

is the value of the cross section calculated for the best (or default) set of parameters $\mathbf{x} = (x_1, \dots, x_j)$ for a specific reaction channel ρ , while

$$\sigma_\rho^{(\pm)}(E, k) = \sigma_\rho^{(\pm)}(E; x_1, x_2, \dots, x_k \pm \delta x_k, \dots, x_j)$$

are cross sections calculated with the value of the parameter k perturbed by its expected uncertainty δx_k . We note, that $\mathcal{S}_\rho(E, k)$ is related to the sensitivity matrix a through

$$\mathcal{S}_\rho(E, k) = 2a_{(E,k)} \delta x_k \quad (5)$$

and is a convenient measure of the cross section response to the physically sensible variation of the model parameter k . Fig. 1 shows examples of such response to the variation of the real depth of the optical potential V_v . The reaction channels plotted in Fig. 1 display remarkably different levels of sensitivity and distinct energy dependence. Fig. 2 shows response of the neutron radiative capture on ^{89}Y to the variation of the dominating parameters. It is obvious that some model parameters generate

Table II. Percentage uncertainties used for the optical model parameters⁵. The subscripts v and s indicate real volume and surface components, while w refers the imaginary surface. The r and a are the radius and diffuseness parameters defining the Wood-Saxon potential, while V and W are the real and imaginary well depths, respectively. 'tg' superscripts indicate neutron plus target (${}^A_Z\text{X}$) channel, while 'np' refers to a proton plus ${}^{A+1}_{Z-1}\text{X}$ system.

	$\Delta r_s^{(tg)}$	$\Delta r_v^{(tg)}$	$\Delta r_w^{(tg)}$	$\Delta V_v^{(tg)}$	$\Delta W_s^{(tg)}$
%	± 3.0	± 3.0	± 3.0	± 3.0	± 5.0
	$\Delta W_v^{(tg)}$	$\Delta a_s^{(tg)}$	$\Delta a_v^{(tg)}$	$\Delta V_v^{(np)}$	$\Delta W_s^{(np)}$
%	± 5.0	± 3.0	± 3.0	± 3.0	± 3.0

small or negligible perturbations on all reaction channels, while others have an important effect only on a specific ones. Two fundamental nuclear reaction mechanisms are clearly evident. In the energy region below 10 MeV, the neutron capture is described by the formation and decay of the compound nucleus. As expected, the nuclear level density parameters a_{cn} and a_{tg} play an important role along with the depths of the real volume V_v and imaginary surface W_s components of optical model potential for neutrons. At higher energies the pre-equilibrium emission mechanism becomes dominant and the mean free path parameter (PE mfp) plays the major role. The radiative strength function enters as a multiplicative factor in all mechanisms, therefore its role is practically constant.

The uncertainties of the model parameters used in the covariance calculations are given in Tabs. II and III. In the case of the optical model, the uncertainties are suggested by the analysis of the Monte Carlo calculations performed by A.J. Koning⁵. Uncertainties for other parameters are estimates resulting from experience and random comparison of the calculated uncertainties with the spread of experimental data. The correlations among model parameters were disregarded. This simplification is justified within the 'low-fidelity' scope of the project, although it ignores some well known physical constraints (e.g., anticorrelation between radius (r_v) and depth (V_v) of the optical potential). Unfortunately, these correlations have not yet been well quantified.

IV. RESULTS

The cross section covariances were calculated for 219 isotopes at 30 incident energies between 5 keV and 20 MeV. The five reaction channels considered in the present exercise were total, elastic, inelastic, capture, and (n,2n). Altogether, 18 model parameters were varied in the calculations. The

Table III. Percentage uncertainties of nuclear level densities \tilde{a} and single particle level densities \tilde{g} (pre-equilibrium emission) parameters. The subscripts relate these quantities to the nuclei - $cn \equiv$ compound, $tg \equiv$ target, $n2n \equiv$ (n,2n) residue, $np \equiv$ (n,p) residue. The uncertainties on the γ -ray strength functions are applied to all nuclei and on those for the pre-equilibrium mean free path apply to the compound (composite) nucleus only.

	$\Delta\tilde{a}^{(cn)}$	$\Delta\tilde{a}^{(tg)}$	$\Delta\tilde{a}^{(n2n)}$	$\Delta\tilde{a}^{(np)}$
%	± 10	± 10	± 10	± 10
	$\Delta\tilde{g}^{(np)}$	$\Delta\tilde{g}^{(tg)}$	$\Delta(\gamma\text{-strength})$	$\Delta(\text{PE mfp})$
%	± 10	± 10	± 20	± 20

results are totally based on model calculations and no experimental data were taken into account. This is in line with the intention of the project which aims to produce low-fidelity covariances for an extensive set of nuclei. The uncertainties were determined following the procedure presented in the Section II. The neutron cross sections were calculated using a default set of model parameters common to all considered nuclei. The covariance matrices were calculated by the KALMAN code and, in explicit notation, they are

$$w_{i,j} = \sum_{\ell,m=1}^J \frac{\partial\sigma(\mathbf{x}; E_i)}{\partial x_\ell} \langle \Delta x_\ell \Delta x_m \rangle \frac{\partial\sigma(\mathbf{x}; E_j)}{\partial x_m}, \quad (6)$$

where $\mathbf{X} \equiv \langle \Delta x_\ell \Delta x_m \rangle$ is the correlation matrix of the model parameters. \mathbf{X} is diagonal, because we assumed them to be uncorrelated with uncertainties given in the Tab. II. The covariance matrices are generally shown in a normalized form,

$$\zeta_{i,j} = \frac{w_{i,j}}{\sqrt{w_{i,i}}\sqrt{w_{j,j}}}, \quad (7)$$

which leads, by definition, to matrix elements in the range $-1 \leq \zeta_{i,j} \leq 1$. We remind that covariance matrices must be symmetric and definite positive, namely

$$\mathbf{Z}\mathbf{W}\mathbf{Z}^T > 0, \quad (8)$$

for all non-zero real vectors. Numerical rounding errors in the normalization procedure expressed by Eq. 7 can lead to inconsistencies and matrices, ζ , not satisfying the condition of Eq. 8.

In Figs. 3-7 relative uncertainties for the most important reaction channels on ^{127}I are shown as an example. The total and elastic channels obviously show a similar structure characterized by the presence of the nodes, where the uncertainties become considerably smaller. This is due to the low sensitivity of the cross sections to the optical potential parameters at these particular energies.

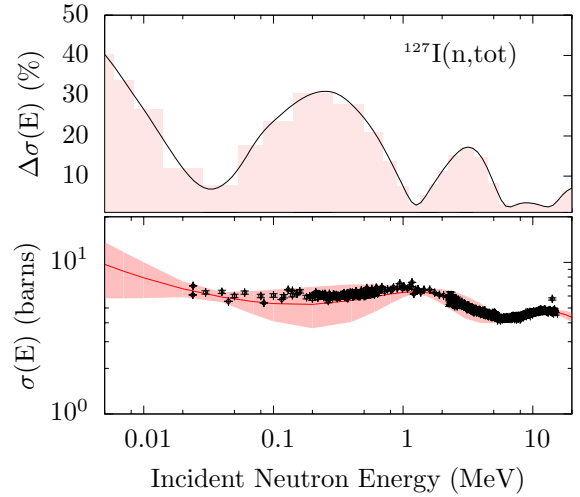


Fig. 3. Relative uncertainties for $^{127}\text{I}(n,\text{tot})$ obtained with the *EMPIRE-KALMAN* method and plotted along with the cross section and experimental data.

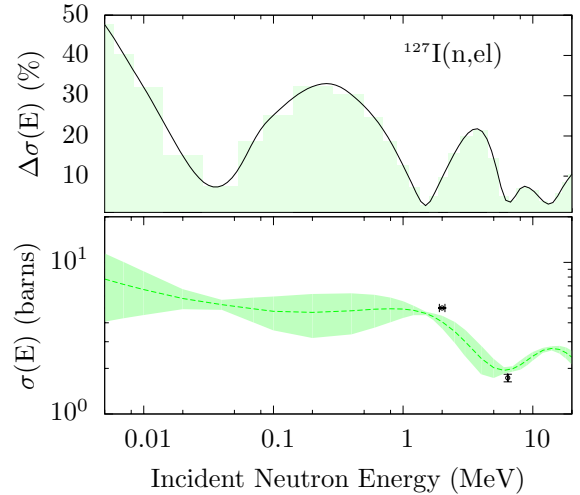


Fig. 4. Relative uncertainties for $^{127}\text{I}(n,\text{el})$ obtained with the *EMPIRE-KALMAN* method and plotted along with the cross section and experimental data.

One can also notice that uncertainties for these two reaction channels become relatively high at low energies and for ≈ 0.5 and ≈ 3 MeV. Inelastic and capture reveal expected high uncertainties for energies ≥ 15 MeV, while, essentially flat shape is obtained for (n,2n) except of the threshold region.

In Figs. 8-12 percentage relative uncertainties for the major reaction channels are shown in a contour plot where the numbers on x and y axes refer to the complete list of fission product nuclei and the number of energy bins respectively.

The exceptionally high uncertainties are found for nuclei between Xe and Eu below 100 keV.

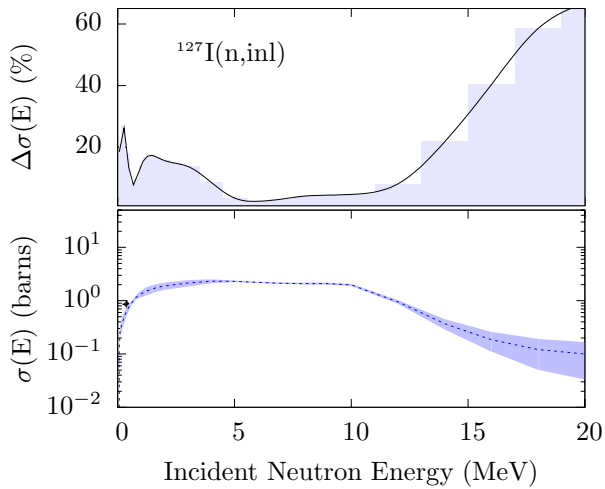


Fig. 5. Relative uncertainties for $^{127}\text{I}(n,\text{inl})$ obtained with the *EMPIRE-KALMAN* method and plotted along with the cross section and experimental data.

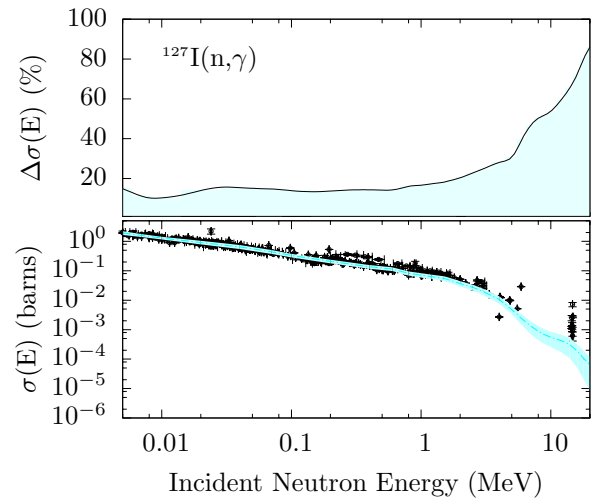


Fig. 7. Relative uncertainties for $^{127}\text{I}(n,\gamma)$ obtained with *EMPIRE-KALMAN* and plotted along with the cross section and experimental data.

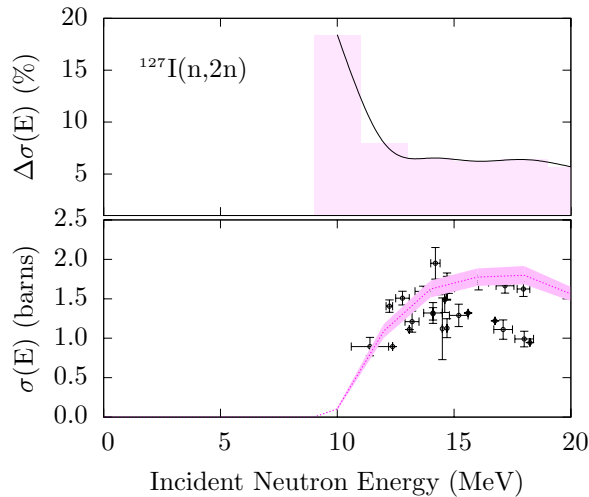


Fig. 6. Relative uncertainties for $^{127}\text{I}(n,2n)$ obtained with the *EMPIRE-KALMAN* and plotted along with the cross section and experimental data.

Possible explanation of this effect can be traced to the structure observed in the s- and/or d-wave neutron strength functions.

V. CONCLUSIONS

We have applied the *EMPIRE-KALMAN* method to determine a consistent set of fast neutron covariance matrices for 219 fission products included in the ENDF/B-VII.0 library. Up to our best knowledge this is the first covariance effort on such a scale. The results are based on model calculations and depend on the assumed uncertainties

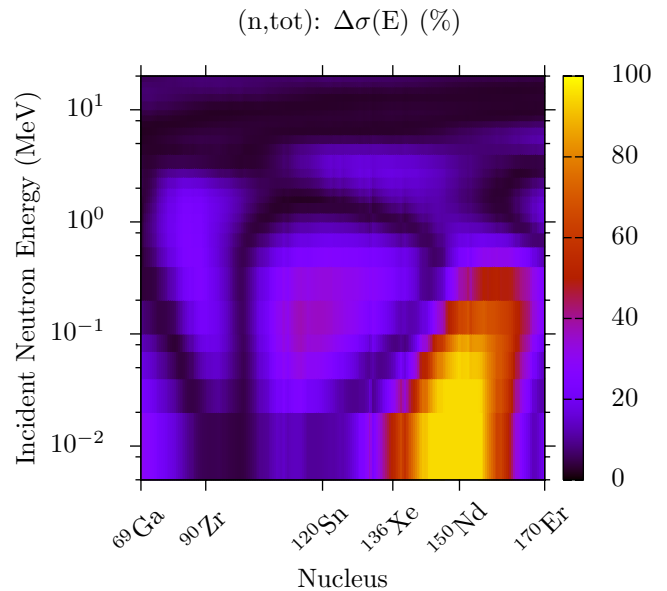


Fig. 8. Relative uncertainties for the total cross sections on 219 fission product materials obtained with the *EMPIRE-KALMAN* method in the fast neutron energy region.

of the model parameters. The experimental data were used globally to ensure that calculated cross section uncertainties are, on average, in reasonable agreement with the spread of measurements and their uncertainties. However, the new covariances are not compatible with the ENDF/B-VII.0 library. Since the same set of model parameters and related uncertainties was used for all 219 nuclides the calculated cross sections and their uncertainties often deviate from the evaluated cross sections and

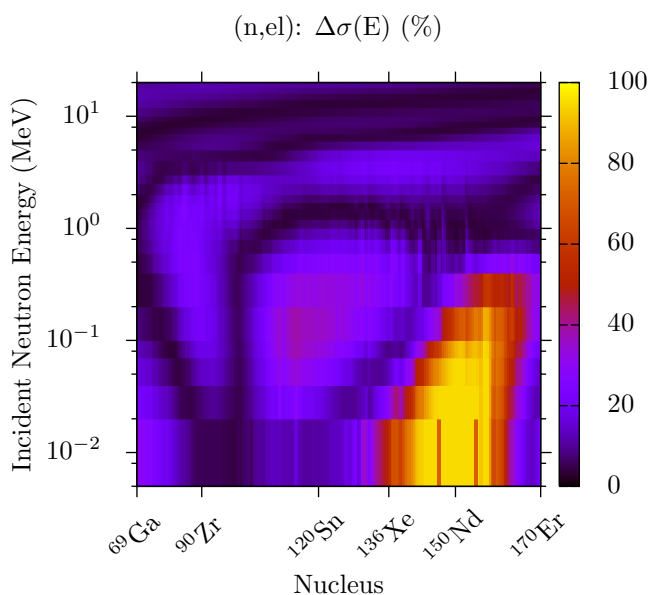


Fig. 9. Relative uncertainties for the elastic cross sections on 219 fission product materials obtained with the *EMPIRE-KALMAN* method in the fast neutron energy region.

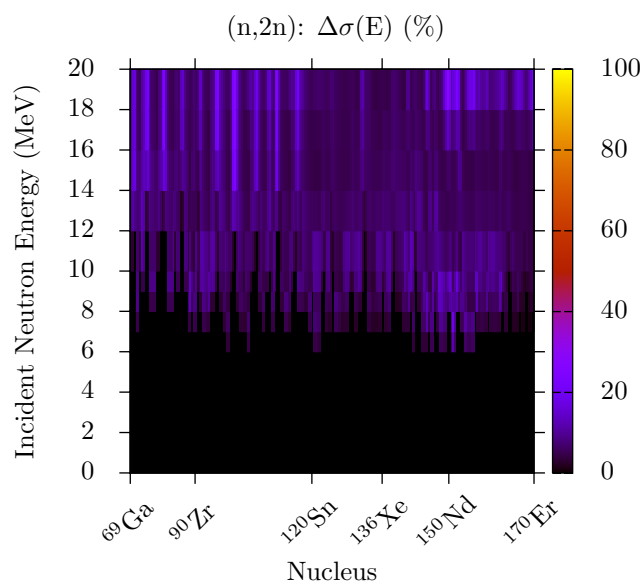


Fig. 11. Relative uncertainties for the (n,2n) cross sections on 219 fission product materials obtained with the *EMPIRE-KALMAN* method in the fast neutron energy region.

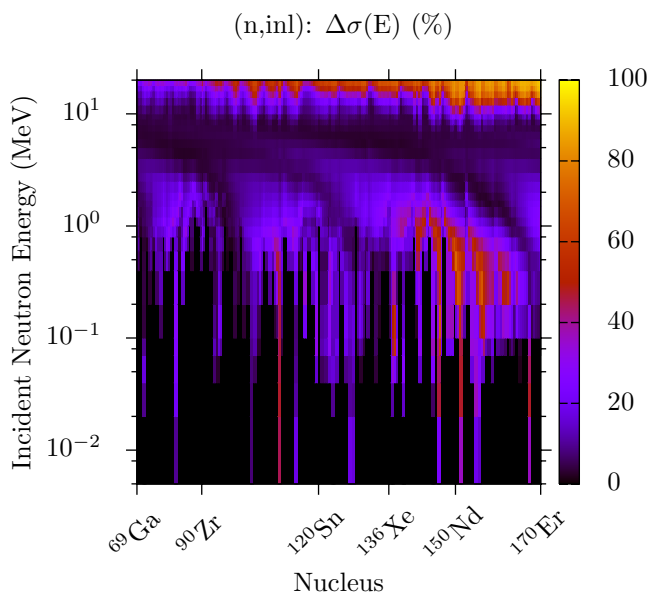


Fig. 10. Relative uncertainties for the inelastic cross sections on 219 fission product materials obtained with the *EMPIRE-KALMAN* method in the fast neutron energy region.

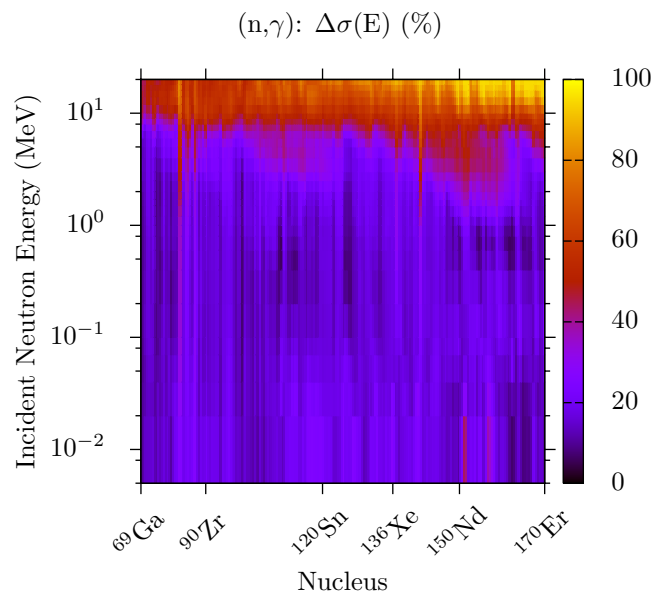


Fig. 12. Relative uncertainties for the capture cross sections on 219 fission product materials obtained with *EMPIRE-KALMAN* method in the fast neutron energy region.

uncertainties derived from the experimental data. This is a natural price to be paid for the global approach, which on the other hand reveals intriguing structure in the uncertainties plotted against incident energy and mass number (the atomic number dependence might also be possible). In particular, we note very similar patterns observed in the total

and elastic channels. A reflection of these patterns is also found in the inelastic one. The (n,2n) and capture channels do not seem to be affected by the structure seen in the total and elastic channels but instead they display short range fluctuations in function of mass number - high and low uncertainties alternate producing vertical lines on the plots. Since

all nuclei were treated on the same footing using the same set of models and default set of parameters, it should be possible to explain the patterns in terms of physics underlying our calculations. For example, the structure showing up in the total and elastic channels arises from the optical model and we understand the origin of deep minima in the cross section uncertainties at certain energies. Mass dependence of the energies at which these minima occur is most likely responsible for creation of the characteristic patterns in Figs. 8 and 9. We are going to address physics background of the observed structures in our future studies.

ACKNOWLEDGMENTS

This work was supported by the DOE-NNSA within the Nuclear Criticality Safety Program. It was partly sponsored by the Office of Nuclear Physics, Office of Science of the U.S. Department of Energy under contract No. DE-AC02-98CH10886 with Brookhaven Science Associates, LLC.

REFERENCES

1. M.B. CHADWICK, P. OBLOŽINSKÝ, M. HERMAN et al., "ENDF/B-VII.0: Next Generation Evaluated Nuclear Data Library for Nuclear Science and Technology", *Nuclear Data Sheets*, **107**, 2931, (2006).
2. D.ROCHMAN, M.HERMAN, P.OBLOŽINSKÝ et al., "Preliminary Cross Section Covariances for WPEC Subgroup 26", BNL-77407-2007-IR (2007).
3. M. HERMAN, R. CAPOTE, B.V. CARLSON et al., "EMPIRE: Nuclear Reaction Model Code System for Data Evaluation", *Nuclear Data Sheets*, to be published (2007).
4. T. KAWANO, K. SHIBATA, "Covariance Evaluation System [in Japanese]", *JAERI-Data/Code*, 97-037 (1997).
5. A.J. KONING, J.P. DELAROCHE, "Local and global nucleon optical models from 1 keV to 200 MeV", *Nucl. Phys. A*, **713**, 213 (2003).